

Dissipation in Pulsar Winds

J. G. Kirk

*Max-Planck-Institut für Kernphysik, Postfach 10 39 80, 69029 Heidelberg,
Germany*

Abstract

I review the constraints placed on relativistic pulsar winds by comparing optical and X-ray images of the inner Crab Nebula on the one hand with two-dimensional MHD simulations on the other. The various proposals in the literature for achieving the low magnetisation required at the inner edge of the Nebula, are then discussed, emphasising that of dissipation in the striped-wind picture. The possibility of direct observation of the wind is examined. Based on the predicted orientation of the polarisation vector, I outline a new argument suggesting that the off-pulse component of the optical emission of the Crab pulsar originates in the wind.

Key words: MHD; pulsars: general; pulsars: Crab; stars: winds, outflows

1 Introduction

Observations of pulsar nebulae have improved dramatically over the past few years. In particular, the X-ray (Weisskopf et al., 2000) and optical (Hester et al., 1995, 2002) images of the Crab Nebula have revealed intriguing insights into the dynamics of this object that have motivated detailed theoretical studies. These, in turn, have sharpened the constraints on the possible physical conditions at the inner boundary of the Nebula, which encloses both the pulsar and an apparently empty region surrounding it. This paper concentrates on the physics of the apparently empty region, that I will call the pulsar *wind*, because it contains out-flowing material, moving, presumably, at supersonic velocity. However, it also contains large amplitude waves of the same period as the pulsar (Rees and Gunn, 1974; Kundt and Krotscheck, 1980) and a substantial dc component of magnetic field (Pacini, 1968).

Whereas the outer boundary of a pulsar wind is, at least in some cases, directly accessible to observation, constraints on the physical conditions where the wind is launched are difficult to find. A common scenario is that the pulsar

magnetosphere drives an almost radial wind that becomes supersonic at some point not too far outside the light cylinder and that contains a current sheet separating the two magnetic hemispheres defined by the dipole component of the field at the stellar surface. However, although this is an attractive model to work on, alternative pictures are possible (e.g., Kuijpers, 2001), because our knowledge of the magnetosphere is incomplete. Even the term *magnetosphere* itself can cause confusion. It is generally used to identify a region in which external electromagnetic fields dominate the dynamics of a plasma. For pulsars, this certainly applies inside the light cylinder. But the definition becomes ambiguous further out, where the magnetic field weakens and the outflow accelerates. This is because electromagnetic fields may still dominate the energy flux even in a supermagnetosonic flow, in which the inertia of the plasma is important. Here, I use the term magnetosphere to refer to regions close to the neutron star where the bulk radial flow is still submagnetosonic, including, of course, those parts within the pulsar light-cylinder that corotate with the star. Understood in this sense, it is generally thought that the wind is dark, but the magnetosphere is responsible for the pulsed emission detected, in the case of the Crab, from the radio to gamma-ray bands as a point source apparently located at the position of the neutron star. As discussed in Section 5 this is not necessarily the case.

In this paper I will briefly review the constraints that can be placed on the physics of the pulsar wind by MHD simulations of the Crab Nebula. I will then consider current theoretical ideas on how these constraints could be met, and finally look at the prospects for observing the wind directly.

2 MHD simulations

Axisymmetric, relativistic MHD simulations of the wind and the bubble it inflates downstream of the termination shock have been performed by Komissarov and Lyubarsky (2003, 2004) and Del Zanna et al. (2004). The results are broadly similar. Provided the energy flux in the wind is assumed to be concentrated towards the equatorial plane, the termination shock is highly oblate — an aspect that had been deduced using analytical arguments by Lyubarsky (2002) and Bogovalov and Khangoulia (2002a,b). If, in addition, the magnetisation parameter $\sigma = B^2/(4\pi w)$ (here B is the magnetic field in the plasma rest frame and w the proper enthalpy density) is tuned to the correct value, then the magnetic pinch in the shocked plasma collimates the flow, as predicted (Lyubarsky, 2002), and a torus-plus-jet like structure similar in appearance to that seen in the optical and X-ray images of the Crab Nebula is reproduced. The anisotropy of the energy flux and the tuning of the magnetisation are critical; the simulations are less sensitive to other parameters such as the Lorentz factor of the flow and the angular distribution of the particle flux.

The anisotropy of the energy flux should follow from the boundary conditions on the magnetic field at the stellar surface. But our knowledge of this connection is scanty. The only known exact solution is that of the force-free split monopole (Michel, 1973). In this case, spherical symmetry of the magnetic field at small radius yields an energy flow per solid angle, $dL/d\Omega$, that is concentrated into the equatorial plane, with a dependence on colatitude θ given by

$$\frac{dL}{d\Omega} \propto \sin^2 \theta \tag{1}$$

The poloidal field in this solution is purely radial, and there are no regions of closed field. Nevertheless, a non-axisymmetric version can be constructed by simply inclining the plane used to “split” the monopole (Bogovalov, 1999). In a realistic case, it is expected that the closed field line regions fill much of the magnetosphere inside the light cylinder [see the discussion in Contopoulos et al. (1999), Uzdensky (2003) and Goodwin et al. (2004)]. Consequently, there is no reason to suppose that the angular distribution given by Eq. (1) is a good approximation. Nevertheless, all simulations published so far start off with essentially this distribution.

There is less consensus concerning the magnetisation parameter σ . This quantity is, in principle, also a function of angle, since it describes the way in which the energy flux at a particular colatitude is divided between Poynting flux and particle-born energy. In the exact force-free solution σ is formally infinite. But a simulation with large σ would fail to look anything like the Crab Nebula. In fact, for σ greater than about 1% in the equatorial region, the jet appears too fast and strong and the equatorial outflow is suppressed. For smaller σ , some of the detailed properties of the outflow match observed features such as the central knot (Hester et al., 1995) quite convincingly (Komissarov and Lyubarsky, 2004). Thus, it appears that the magnetisation parameter must be very small in the equatorial wind. This is a well-known and puzzling property, as discussed below. It is sometimes termed the “ σ paradox”, and was already recognised in spherically symmetric models of the Crab Nebula (Kennel and Coroniti, 1984). On the other hand, if σ is everywhere small, the two-dimensional simulations resemble the purely hydrodynamical case, resulting in a “lonely torus” (Komissarov and Lyubarsky, 2004).

The value of σ in the energetically less important, polar parts of the outflow is uncertain. Del Zanna et al. (2004) concentrate on the case in which σ is independent of angle, with a current sheet in the equatorial plane, as in the case of the “aligned” split monopole. On the other hand, Komissarov and Lyubarsky (2003, 2004) are motivated by the scenario where low magnetisation is achieved by complete dissipation of the oscillating component of the magnetic field in the “striped wind” of the oblique split-monopole solution (Coroniti, 1990;

Fig. 1. The striped pulsar wind. A magnetic dipole embedded in the star at an oblique angle to the rotation axis introduces field lines of both polarities into the equatorial plane. The figure shows the intersection of the current sheet separating these regions and the equatorial plane. In the inset, an almost planar portion of this sheet (dashed line) is shown, together with the magnetic field lines, assuming they undergo reconnection.

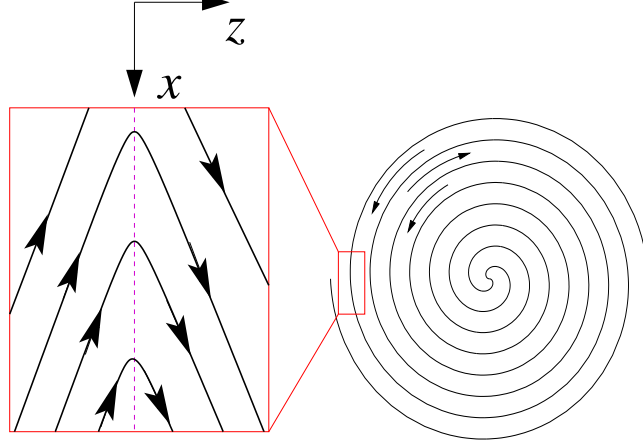


Table 1

Dependence of the bulk Lorentz factor Γ of the pulsar wind on radius for different dissipation mechanisms. r_{\max} is the radius at which dissipation is complete, r_L is the radius of the light-cylinder, $\mu = L/(\dot{N}_{\pm} mc^2)$ is Michel's parameter (with L the spin-down luminosity, and \dot{N}_{\pm} the pair loss rate in the wind) and $\hat{L} = L\pi^3 e^2 / (m^2 c^5 \Omega_w)$ is a dimensionless measure of the spin-down luminosity divided by the solid angle Ω_w occupied by the wind ($\hat{L} \approx 1.5 \times 10^{22}$ for the Crab pulsar). \hat{L} is approximately equal to the square of the pole to equator potential in units of the electron rest-mass.

Slow dissipation	Tearing-mode	Fast dissipation
$\Gamma \propto r^{1/2}$	$\Gamma \propto r^{5/12}$	$\Gamma \propto r^{1/3}$
$r_{\max}/r_L = \hat{L}^{1/2}$	$r_{\max}/r_L = \mu^{4/5} \hat{L}^{3/10}$	$r_{\max}/r_L = \mu^2$

Lyubarsky and Kirk, 2001). On the equator, the dc component of the field in this solution vanishes for all obliquities, and so $\sigma = 0$ here after dissipation of the stripes. But, for all except the exactly perpendicular case, the stripes are confined to a band of latitudes around the equator, implying a high value of σ close to the poles. Interestingly, both groups agree that the average value of σ , i.e., the ratio of the total luminosity in Poynting flux to the total in particle-born flux, should be a few percent.

3 The σ paradox

The exact solution with $\sigma \rightarrow \infty$ found by Michel (1973) has radial poloidal field. Its large σ counterpart also appears neither to collimate significantly, nor to accelerate (Bogovalov and Tsinganos, 1999). Thus, if, as expected, σ is large close to the star, it should continue to be so out to the termination shock. The small magnetisation implied by observations completes the σ paradox.

There are several possible escape routes:

- (1) Before the advent of the high-resolution images of the Crab Nebula, Begelman (1998) suggested that σ remains large even outside the termination shock, and that the magnetic energy dissipates in the Nebula. However, this now seems to be ruled out by the good agreement of low σ , ideal MHD simulations and observations in the optical and X-ray bands.
- (2) Lyubarsky (2003b) also proposed that σ remains large in the wind, but that the energy carried in the oscillating component of the magnetic field dissipates in a transition region that can be considered as a special kind of termination shock. Such a configuration leads to the same initial conditions for the MHD simulations as does a low σ wind, provided the transition region remains thin. This is an interesting suggestion that needs further investigation. In particular, it would be important to identify any spectral signature that could depend on the position of the termination shock.
- (3) Some collimation and, therefore, acceleration and conversion of magnetic into particle-born energy might be possible if the initial distribution of poloidal flux is sufficiently anisotropic (Chiueh et al., 1998; Vlahakis, 2004). However, whether this is a realistic possibility can only be determined by constructing a model of the inner magnetosphere.
- (4) Coroniti (1990) and Michel (1994) proposed that the oscillating component of the magnetic field in the striped wind picture should gradually damp by dissipation of the magnetic energy at the field line reversals. However, these early papers did not include the associated acceleration of the wind and the resulting dilation of the dissipation timescale.

Routes (2) and (3) await further theoretical development, and I now turn to a discussion of route (4).

4 Dissipation mechanisms

To assess the importance of wave damping as a possible solution of the σ problem it is first necessary to identify the nature of the wave. Close to the pulsar,

electromagnetic modes do not propagate (Usov, 1975; Melatos and Melrose, 1996). On the other hand, both the fast magnetosonic wave (Lyubarsky, 2003a) and the entropy wave (Lyubarsky and Kirk, 2001) are possible. In principle, these may convert spontaneously into electromagnetic modes at larger radius (Melatos, 1998), but the conditions under which this happens have not yet been fully investigated. If the waves persist as subluminal modes, damping is inevitable (Usov, 1975).

The rate of damping of the striped wind pattern and, therefore, the viability of escape route (4), depends on the speed with which magnetic reconnection can proceed in a relativistic current sheet. These structures (see Fig. 1) differ from their more familiar counterparts in solar and magnetospheric physics because they do not permit evacuation of the heated plasma from the sheet as in a Sweet-Parker or Petschek-type reconnection model (Kirk, 2004). Instead, either the sheet steadily thickens, or plasma is ejected along the induced electric field (the \vec{y} -direction in Fig. 1). As dissipation proceeds, the current sheet separating regions of opposite magnetic polarity fills with hot plasma. If this process proceeds slowly (not faster than the timescale needed for a fluid element in the wind to double its radius) a small-wavelength approximation can be used to analyse the evolution of the stripes. On the other hand, rapid dissipation cannot be ruled out, and is difficult to quantify.

Concentrating on the small-wavelength approximation, the physical picture is one in which the sheet remains in approximate pressure equilibrium with the surrounding magnetic field, which is dragged into it and annihilated. Spherical symmetry must be assumed to make the analysis tractable, but since the flow is highly relativistic, pressure imbalance in the θ direction is unlikely to be important, and we can assume the solution holds independently along each radius vector. A lower limit on the rate at which annihilation can proceed is found by arguing that the sheet width cannot be smaller than the gyro radius of a “hot” particle in the confining field (Lyubarsky and Kirk, 2001). However, this rate is too slow to be of interest in the case of the Crab. A more realistic estimate of the annihilation rate follows by assuming it equals the timescale on which the relativistic tearing-mode instability operates (Lyubarskii, 1996; Kirk and Skjæraasen, 2003). But, again, this is not fast enough to resolve the σ paradox for the Crab. An upper limit, subject to the assumptions inherent in this method, is given by demanding that the hot sheet expand at most sonically. This *does* provide a viable escape route for the case of the Crab, but only if the number of electron/positron pairs carried from the pulsar by the wind is significantly larger ($> 3 \times 10^{40} \text{ s}^{-1}$) than the rate found in standard pair-production calculations (Hibschman and Arons, 2001a,b). Independent support for injection of pairs into the Nebula at this high rate is provided by models of the radio to hard X-ray synchrotron spectrum (Gallant et al., 2002), so that we may still have much to learn about where and how a pulsar produces electron/positron pairs.

For each of these proposed dissipation processes, the acceleration of the wind can be described by a similarity solution in which the bulk Lorentz factor is proportional to a power of the radius. These results are summarised in Table 1. In principle, they make possible a prediction of both the average σ and the Lorentz factor of a pulsar wind as a function of radius. Given the inclination angle of the magnetic dipole axis, predictions can also be made of the dependence of these quantities on colatitude.

5 Observing the wind

In the case of gamma-rays, an observational upper limit on the wind emission yields a firm constraint on the pulsar wind. Even if the plasma remains completely cold, if its bulk Lorentz factor is large, it will radiate by Compton upscattering the ambient target photons. Using thermal X-rays from the surface of the Crab pulsar as targets, Bogovalov and Aharonian (2000) interpreted the detected unpulsed flux in TeV gamma-rays as an upper limit on the contribution of the wind, and derived a *lower* limit of $5r_L$ on the radius at which the Lorentz factor of the Crab wind can reach 10^6 . This constraint is satisfied by all the models presented in Table 1.

In the optical and X-ray images the region around the Crab pulsar appears dark out to a distance of about 12 arcsec. However, this does not mean the wind does not radiate, but merely that along a line of sight that passes between about 0.5 arcsec and 12 arcsec of the pulsar, the emission of the wind is beamed away from the observer. This occurs quite naturally in a relativistic, radial wind. If the bulk Lorentz factor is proportional to r^q with $q < 1$ — as in the cases considered in Table 1 — the most stringent constraint is imposed at the termination shock. For the emission to be beamed away from the observer at that radius requires $\Gamma > 12 \text{ arcsec} / 0.5 \text{ arcsec} = 24$. This is much smaller than the Lorentz factor usually assumed for the plasma entering the termination shock. Consequently, even if it radiates at all radii, the wind should appear to contribute only to the point source, leaving the surrounding region dark.

An analogous argument can be advanced concerning pulsation of the wind emission. If the striped pattern gives rise to a phase dependence of the emissivity, for example, to increased emission at the field reversals, the radiation from radius r will appear pulsed at the rotation period of the star provided $r/r_L < \Gamma^2$ (Kirk et al., 2002).

Has this radiation been observed? To answer this question, one must be able to untangle the contribution of the stellar surface, magnetosphere and wind, all of which are co-spatial (and point-like) when observed with current instruments. This is a difficult task, especially given the uncertainties associated with mod-

elling the pulsed emission. However, one characteristic of synchrotron emission from the wind that does not appear to be shared by any magnetospheric model (Dyks et al., 2004; Kaspi et al., 2004) is the direction of linear polarisation of the off-pulse or “dc” component. In the striped wind, the polarisation vector of radiation emitted close to the field reversals is not well constrained, but outside of these potentially pulse-producing regions, the magnetic field is purely toroidal. This predicts that the electric vector of the dc component of synchrotron radiation should lie along the projection onto the sky of the rotation axis of the neutron star. In the case of the Crab pulsar, the optical emission appears to have precisely this property (Kellner, 2002).

Acknowledgements

I thank Gottfried Kanbach for discussions of the optical emission of the Crab pulsar

References

- Begelman, M. C., 1998. Instability of Toroidal Magnetic Field in Jets and Plerions. *ApJ*493, 291–300.
- Bogovalov, S., Tsinganos, K., 1999. On the magnetic acceleration and collimation of astrophysical outflows. *MN*305, 211–224.
- Bogovalov, S. V., 1999. On the physics of cold MHD winds from oblique rotators. *A&A*349, 1017–1026.
- Bogovalov, S. V., Aharonian, F. A., 2000. Very-high-energy gamma radiation associated with the unshocked wind of the Crab pulsar. *MN*313, 504–514.
- Bogovalov, S. V., Khangoulia, D. V., 2002a. On the origin of the torus and jet-like structures in the centre of the Crab Nebula. *MN*336, L53–L55.
- Bogovalov, S. V., Khangoulia, D. V., 2002b. The Crab Nebula: Interpretation of Chandra Observations. *Astronomy Letters* 28, 373–385.
- Chiueh, T., Li, Z., Begelman, M. C., 1998. A Critical Analysis of Ideal Magnetohydrodynamic Models for Crab-like Pulsar Winds. *ApJ*505, 835–843.
- Contopoulos, I., Kazanas, D., Fendt, C., 1999. The Axisymmetric Pulsar Magnetosphere. *ApJ*511, 351–358.
- Coroniti, F. V., 1990. Magnetically striped relativistic magnetohydrodynamic winds - The Crab Nebula revisited. *ApJ*349, 538–545.
- Del Zanna, L., Amato, E., Bucciantini, N., 2004. Axially symmetric relativistic MHD simulations of Pulsar Wind Nebulae in Supernova Remnants. On the origin of torus and jet-like features. *A&A*421, 1063–1073.
- Dyks, J., Harding, A. K., Rudak, B., 2004. Relativistic Effects and Polarization in Three High-Energy Pulsar Models. *ApJ*606, 1125–1142.

- Gallant, Y. A., van der Swaluw, E., Kirk, J. G., Achterberg, A., 2002. Modeling Plerion Spectra and their Evolution. In: ASP Conf. Ser. 271: Neutron Stars in Supernova Remnants. p. 161.
- Goodwin, S. P., Mestel, J., Mestel, L., Wright, G. A. E., 2004. An idealized pulsar magnetosphere: the relativistic force-free approximation. *MN*349, 213–224.
- Hester, J. J., Mori, K., Burrows, D., Gallagher, J. S., Graham, J. R., Halverson, M., Kader, A., Michel, F. C., Scowen, P., 2002. Hubble Space Telescope and Chandra Monitoring of the Crab Synchrotron Nebula. *ApJ*577, L49–L52.
- Hester, J. J., Scowen, P. A., Sankrit, R., Burrows, C. J., Gallagher, J. S., Holtzman, J. A., Watson, A., Trauger, J. T., Ballester, G. E., Casertano, S., Clarke, J. T., Crisp, D., Evans, R. W., Griffiths, R. E., Hoessel, J. G., Krist, J., Lynds, R., Mould, J. R., O’Neil, E. J., Stapelfeldt, K. R., Westphal, J. A., 1995. WFPC2 Studies of the Crab Nebula. I. HST and ROSAT Imaging of the Synchrotron Nebula. *ApJ*448, 240–263.
- Hibschman, J. A., Arons, J., 2001a. Pair Multiplicities and Pulsar Death. *ApJ*554, 624–635.
- Hibschman, J. A., Arons, J., 2001b. Pair Production Multiplicities in Rotation-powered Pulsars. *ApJ*560, 871–884.
- Kaspi, V. M., Roberts, M. S. E., Harding, A. K., 2004. Isolated neutron stars. In: astro-ph/0402136.
- Kellner, S., 2002. Master’s thesis, Technische Universität München.
- Kennel, C. F., Coroniti, F. V., 1984. Confinement of the Crab pulsar’s wind by its supernova remnant. *ApJ*283, 694–709.
- Kirk, J. G., 2004. Particle Acceleration in Relativistic Current Sheets. *Physical Review Letters* 92 (18), 181101–181104.
- Kirk, J. G., Skjæraasen, O., 2003. Dissipation in Poynting-Flux-dominated Flows: The σ -Problem of the Crab Pulsar Wind. *ApJ*591, 366–379.
- Kirk, J. G., Skjæraasen, O., Gallant, Y. A., 2002. Pulsed radiation from neutron star winds. *A&A*388, L29–L32.
- Komissarov, S. S., Lyubarsky, Y. E., 2003. The origin of peculiar jet-torus structure in the Crab nebula. *MN*344, L93–L96.
- Komissarov, S. S., Lyubarsky, Y. E., 2004. Synchrotron nebulae created by anisotropic magnetized pulsar winds. *MN*349, 779–792.
- Kuijpers, J., 2001. Equatorial Pulsar Winds. *Publications of the Astronomical Society of Australia* 18, 407–414.
- Kundt, W., Krotscheck, E., 1980. The Crab nebula - A model. *A&A*83, 1–2.
- Lyubarskii, Y. E., 1996. A model for the energetic emission from pulsars. *A&A*311, 172–178.
- Lyubarsky, Y., Kirk, J. G., 2001. Reconnection in a Striped Pulsar Wind. *ApJ*547, 437–448.
- Lyubarsky, Y. E., 2002. On the structure of the inner Crab Nebula. *MN*329, L34–L36.
- Lyubarsky, Y. E., 2003a. Fast magnetosonic waves in pulsar winds. *MN*339, 765–771.

- Lyubarsky, Y. E., 2003b. The termination shock in a striped pulsar wind. MN345, 153–160.
- Melatos, A., 1998. The ratio of Poynting flux to kinetic-energy flux in the Crab pulsar wind. *Memorie della Societa Astronomica Italiana* 69, 1009–1015.
- Melatos, A., Melrose, D. B., 1996. Energy transport in a rotation-modulated pulsar wind. MN279, 1168–1190.
- Michel, F. C., 1973. Rotating Magnetospheres: an Exact 3-D Solution. ApJ180, L133–L137.
- Michel, F. C., 1994. Magnetic structure of pulsar winds. ApJ431, 397–401.
- Pacini, F., 1968. Rotating neutron stars, pulsars and supernova remnants. *Nature* 219, 145.
- Rees, M. J., Gunn, J. E., 1974. The origin of the magnetic field and relativistic particles in the Crab Nebula. MN167, 1–12.
- Usov, V. V., 1975. Wave zone structure of NP 0532 and infrared radiation excess of Crab Nebula. *Astrophys. & Space Sci.*32, 375–377.
- Uzdensky, D. A., 2003. On the Axisymmetric Force-free Pulsar Magnetosphere. ApJ598, 446–457.
- Vlahakis, N., 2004. Ideal Magnetohydrodynamic Solution to the σ Problem in Crab-like Pulsar Winds and General Asymptotic Analysis of Magnetized Outflows. ApJ600, 324–337.
- Weisskopf, M. C., Hester, J. J., Tennant, A. F., Elsner, R. F., Schulz, N. S., Marshall, H. L., Karovska, M., Nichols, J. S., Swartz, D. A., Kolodziejczak, J. J., O’Dell, S. L., 2000. Discovery of Spatial and Spectral Structure in the X-Ray Emission from the Crab Nebula. ApJ536, L81–L84.